Geological Society of America Bulletin

Numerical modeling of the development of U-shaped valleys by glacial erosion

JONATHAN M. HARBOR

Geological Society of America Bulletin 1992;104;1364-1375
doi:10.1130/0016-7606(1992)104<1364:NMOTDO>2.3.CO;2

Notes

Numerical modeling of the development of U-shaped valleys by glacial erosion

JONATHAN M. HARBOR* *Department of Geological Sciences and Quaternary Research Center, University of Washington, Seattle, Washington 98195*

ABSTRACT

The steep-sided valleys and overdeepened basins of alpine landscapes are well-known products of glaciation, yet relatively little is known about how the dynamics of ice flow and glacial erosion interact to give rise to such landforms. By linking a finite-element model for ice flow through a glacier cross section with an erosion model, it is possible to investigate the development of one of the most striking glacial landforms, the U-shaped valley. In addition to providing a detailed understanding of landform development, such modeling provides a way to test current understanding of the controls on glacial sliding and erosion.

To simulate valley development, I first model flow through an initial glacier cross section and calculate the glaciological parameters that govern erosion. I then numerically simulate erosion to produce a modified transverse profile, for which a new flow field and erosion pattern are computed. A number of iterations permits examination of the progressive transformation of cross-section form, which can be compared with field data.

Model predictions of the cross-section flow field are in close accord with data from the Athabasca Glacier and include marked lateral variations in sliding velocity. With an erosion law dependent on basal velocity, the model predicts the rapid transformation of a V-shaped cross section into a recognizably glacial form over a time period on the order of 10^4 yr and the eventual development of a steady-state, quasi-parabolic glacier cross section. Better agreement with empirical data from glaciated valleys is obtained by including temporal variations in ice discharge, in order to mimic the characteristics of 100,000-yr glacial cycles. The high-discharge phase dominates form development, and, at low discharges, cross-section form is essentially inherited from the central part of the form that developed during the preceding high-discharge phase.

INTRODUCTION

The U-shaped valley is one of the most well-known products of alpine glaciation, yet relatively little is known about the way in which ice flow and glacial erosion interact in the development of this characteristic form. Although empirical studies have confirmed the general notion that many glaciated valleys have approximately parabolic (U-shaped) cross sections (Svennson, 1958, 1959; Graf, 1970; Doornkamp and King, 1971; Girard, 1976; Aniya and Welch, 1981; Aniya and Naruse, 1985), a convincing explanation of why glacial erosion should produce such a form and why U-shaped valleys are so common in glaciated mountains has only begun to emerge in the past two decades (Johnson, 1970; Boulton, 1974; Roberts and Rood, 1984; Harbor and others, 1988; Harbor, 1990a). Recognizing that conversion of a V-shaped to a U-shaped valley requires valley widening and, more specifically, maximum net erosion part way up the valley walls (Matthes, 1930), the primary emphasis in most early process studies was on evaluating mechanisms that might give rise to maximum erosion at the edge of a glacier (Chamberlin and Chamberlin, 1911; Crosby, 1928; Lewis, 1947; Glen and Lewis, 1961; Embleton and King, 1968). General explanations of the development of U-shaped valleys, however, have typically been couched either in terms of an analogy with stream channels (Gannett, 1898; Davis, 1900, 1906; Charlesworth, 1957) or some general notion that the form evolves to provide maximum efficiency for ice flow through the section (Flint, 1947; Hirano, 1981; Hirano and Aniya, 1988, 1989; and discussed in Harbor, 1990b, and Hirano and Aniya, 1990).

More recent attempts to apply a detailed understanding of flow and erosion mechanics to problems of glacial landform development illustrated the potential importance of feedbacks between flow and erosion patterns in the development of valley forms (for example, Nye and Martin, 1967; Johnson, 1970; Boulton, 1974; Roberts and Rood, 1984), but these attempts relied in part on conceptual models of ice flow and glacial erosion that do not reflect current understanding in these areas. In addition, these studies typically used flow and erosion solutions for end-member forms to provide the basis for descriptive accounts of what might have occurred at intermediate stages (Johnson, 1970; Boulton, 1974; Roberts and Rood, 1984), whereas it is now possible to develop iterative models that explicitly examine progressive form evolution (for example, Oerlemans, 1984).

In the past two decades, the development of numerical ice-flow models that include realistic ice rheology and basal sliding has dramatically improved our ability to simulate the characteristics of glacier motion (Reynaud, 1973; Budd and Jensen, 1975; Mahaffy, 1976; Hooke and others, 1979; Iken, 1981; Bindschadler, 1982; Oerlemans, 1984; Hodge, 1985; Harbor, 1992), whereas theoretical and empirical work in geomorphology has significantly advanced our understanding of glacial erosion processes at small scales (Hallet, 1979, 1981; Röthlisberger and Iken, 1981; Shoemaker, 1988; Iverson, 1990, 1991). In work presented in its early stages in Harbor and others (1988), and in detail here, these advances are used to develop a process-based explanation for the transformation of V-shaped valleys to U-shaped valleys as a result of glacial erosion. This work makes use of a numerical model that simulates ice flow and erosion in a glacier cross section to examine the complex feedbacks between flow patterns, erosion patterns, and cross-section form development that are central to understanding the progressive development of U-shaped valleys. In addition, by calibrating the model with reasonable rates of glacial erosion, it is possible to provide initial estimates for the time scale involved

*Present address: Department of Geology, Kent State University, Kent, Ohio 44242.

Geological Society of America Bulletin, v. 104, p. 1364–1375, 13 figs., 2 tables, October 1992.

in the development of U-shaped valleys, which are key to explaining why these forms are so abundant in glaciated mountains.

DEFINITIONS AND INITIAL ASSUMPTIONS

To facilitate subsequent discussion, I define the following terms used in describing valley cross sections (see also Fig. 1).

Glacial Valley: a valley in which there is a glacier at the time of interest. This includes not only the area in contact with glacier ice but also the side slopes up to the drainage divide, regardless of whether these have been affected by glacial action in the past.

Glaciated Valley: a valley formerly occupied by a glacier. For the cross section, this includes not only the area affected by glacial action in the past but also the side slopes up to the drainage divide.

Active Glacial Channel: the area of the valley actually in contact with a glacier at the time of interest.

Zone of Glacial Influence: the area of the valley within the maximum ice limit. This zone defines the area that was directly affected by glacial action in the past, regardless of whether this area has subsequently been modified by nonglacial processes. This term may be modified to reflect areas affected by a particular period of glaciation (for example, the late Wisconsinan zone of glacial influence).

The need for these definitions was suggested mainly by some initial simulation results (Harbor and others, 1988) which highlighted the fact that progressive vertical erosion can result in a final *zone of glacial influence* significantly different from the *active glacial channel* at the time of maximum ice extent (Fig. 1). The terminology avoids the possible implication that the zone of glacial influence also represents the form of the ice-contact surface at the period associated with the maximum ice limit.

The most basic assumption underlying the work presented here is that the forms of glaciated valleys result primarily from differential glacial erosion controlled by patterns of ice flow. Although the initial preglacial form of the valley is controlled by subaerial processes, I do not consider the evolution of valley forms as a result of subaerial processes (Augustinus, 1988), and, although the influence of patterns of bedrock resistance on form development is considered in Augustinus (1988, 1992) and Harbor (1990a), alternate explanations that view glacial landform evolution primarily in terms of the development of specific patterns of bedrock resistance (Lewis, 1954; Tricart and Cailleux, 1962; Linton, 1963) are not evaluated in this study.

MODEL STRUCTURE

The core of the cross-section development model (Fig. 2) is a finite-element program developed by Charlie Raymond at the University of Washington, which calculates the flow pattern for any given glacier cross section using equations describing ice deformation and basal sliding (Raymond, 1978; Harbor, 1992). This flow program is used to calculate the flow pattern for some initial glacier cross section (typically a preglacial V-shaped valley), and the glaciological information this provides is then combined with a general law for glacial erosion to calculate the pattern of erosion across the profile. For some given time interval, the model then calculates how the shape of the section will change and derives coordinates for new glacier and valley cross sections. This new glacier cross section is used as the next initial condition, and, in this way, the model sets up an iterative framework to study the progressive evolution of the glacial valley. It is this framework, with successive small adjustments of form to flow patterns via the erosion law, and vice versa, that allows for a close examination of the interactions between ice flow, erosion patterns, and form development during the evolution of glacial valleys (Fig. 2). Although a detailed description of the model is provided in Harbor (1990a), certain critical parts of the model are discussed briefly below.

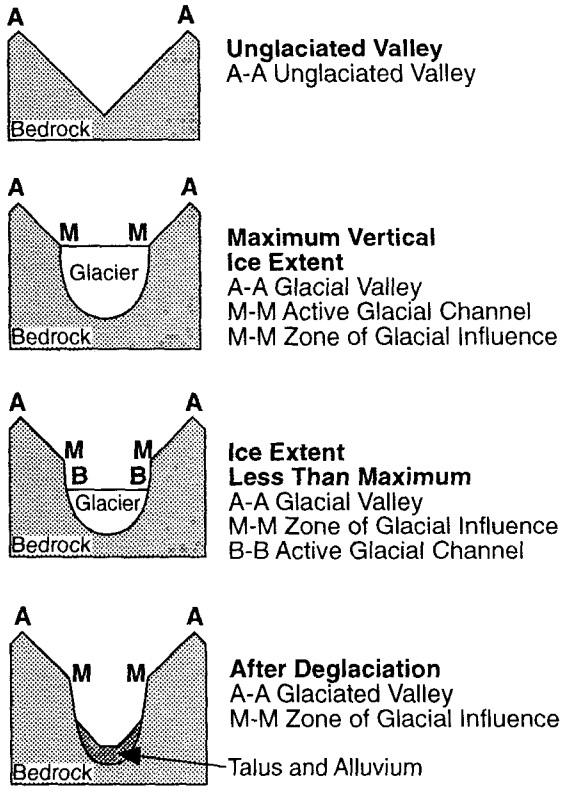

Figure 1. Schematic evolution of a valley as a result of glacial erosion, illustrating the terminology used herein to describe critical regions of the cross section.

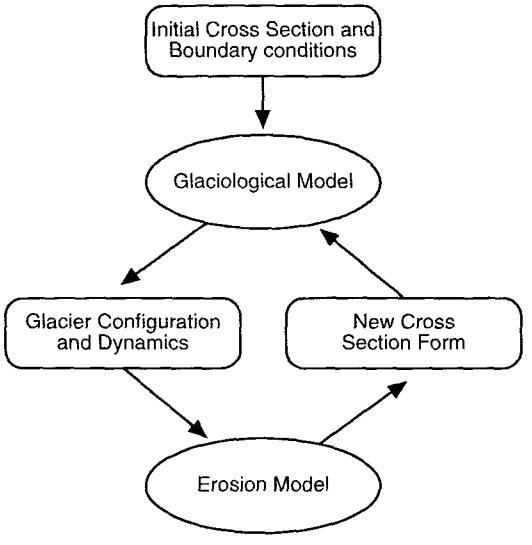

Figure 2. General structure of the landform-development model. Rectangular elements represent inputs and outputs; oval elements represent computational components.

The Initial Glacier Cross Section

Although almost any initial cross-section form can be specified in the model, in the simulations described here, a V-shaped section was selected as the starting condition because it is often described as the "typical" product of processes dominant in temperate areas, and in many other studies of glacial valley development, an initial V-shaped form was assumed (McGee, 1883, 1894; Matthes, 1930; Johnson, 1970; Boulton, 1974). The initial condition is typically unimportant for the long-term evolution of valley form, however. The model assumes that the V-shape form continues above the glacier to whatever extent is needed in the simulations, that is, the glacier never overflows its valley.

Flow Modeling

The glaciological model consists of a finite-element calculation of the pattern of flow for a power-law fluid in an inclined channel, assuming the flow is rectilinear. It is assumed that the ice is at melting point throughout and that the strain rate is proportional to the stress raised to a power of ~3, following Glen's flow law (Glen, 1952, 1955). Basal sliding is modeled as a function of the basal shear stress (τ_b) and the effective normal stress (N) (Lliboutry, 1968, 1979; Raymond, 1971; Budd and others, 1979; Raymond and Harrison, 1987):

$$U_b = k\,\tau_b^{m}\,N^{-p}, \qquad (1)$$

where U_b is the basal sliding velocity, m and p are positive constants, and k is a sliding parameter related to bed roughness and structure. The effective normal stress (N) is the difference between the ice overburden and the basal water pressure and, assuming a level piezometric surface for the cross section, N is zero at the margin, rises to a maximum where the piezometric surface intersects the bed, and then decreases progressively toward the center of the section (Raymond, 1971; Reynaud, 1973; Bindschadler, 1983; Harbor, 1990b, 1992; Fig. 3).

A calibrated version of the glaciological model has successfully been used to predict the main characteristics of the flow pattern observed at a cross section of the Athabasca Glacier by Raymond (1971) (Harbor, 1992); in particular, it predicts significant spatial variations in basal sliding velocities, from very high values near the center of the section to negligible values at the margins. This is an important characteristic of the flow pattern, as conditions at the ice/bedrock interface provide one of the primary controls for rates of glacial erosion.

Erosion Modeling

Glacial erosion consists of several processes, including abrasion, plucking (also known as quarrying), subglacial fluvial erosion, and chemical dissolution by subglacial water. Although the highly complex nature of these mechanisms and the difficulty of examining conditions at glacier beds has largely precluded the development of complete physical models for these processes, empirical and theoretical analyses have provided some indication of the primary controls on rates of glacial erosion (see, for example, the review in Drewry, 1986). In the simulations described here, net erosion normal to the bedrock surface (E) is calculated as

$$E = ec\,T\,U_b^{ev} \qquad (2)$$

where ec is an erosion constant; T is the time-step size; U_b is the sliding velocity; and ev is an erosion exponent. The model is set up to include dependences on effective normal stress and basal shear stress in the erosion equation, but equation 2 is used here because it represents the general form of the abrasion law proposed by Hallet (1979) and more generally applies to *any* process or combination of processes for which erosion scales primarily with basal velocity (see, for example, Shoemaker, 1986). Boulton's (1974) model for abrasion was not used here because of concerns that it may include a physically unrealistic expression for the contact force between a basal clast and the underlying bedrock (Hallet, 1979).

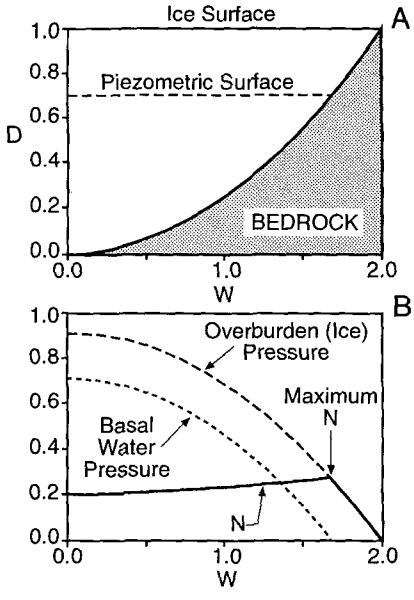

Figure 3. Effective normal stress distribution for a glacier with a parabolic cross section. Part A is a section through one-half of a glacier with a parabolic bed profile and a horizontal piezometric surface. D and W are dimensionless vertical and horizontal distances, respectively, from the low point of the section. Part B shows the distribution of the effective normal stress (N) for this section, where N is simply the overburden pressure minus the basal water pressure. Note that N increases rapidly away from the glacier margin to a maximum value, and then decreases progressively toward the center of the section.

Time-Scale Calculations

The erosion constant (ec in equation 2) is used primarily in calibrating the model against known or specified erosion rates, and thus it directly affects the time scale for form evolution in the model. The erosion constant is effectively a measure of bedrock resistance to erosion, and thus it can be varied both within and between cross sections to reflect complex spatial variations in lithology at a range of scales. Current theoretical and empirical work has yet to produce an accurate way to derive values for ec; there exist general estimates of average erosion rates for some glaciers, but this information is not ideal, because erosion rates generally are not tied to specific values of U_b. The primary exceptions to this are data from the Variegated Glacier, Glacier d'Argentiere, and Breidamerkurjokull presented in Humphrey (1987) which suggest that for $ev = 1.0$, ec is on the order of 10^{-4} over a wide range of velocities (that is, erosion rates of less than a millimeter to several centimeters per year for a typical range of glacier velocities).

Given the difficulty in specifying values for ec, the model is set up to address the time-scale problem in three alternate ways. In the first option, the user specifies a value for ec, presumably derived from unspecified theoretical considerations or empirical data. In the second option, no value for ec is specified, and so, rather than using absolute-time units, the model results are expressed in dimensionless, relative-time units (time steps). In

the third option, the user specifies the average cross-sectional erosion rate for the initial condition, and the model calculates the value of *ec* required to produce this initial erosion rate.

In many of the simulations described here, option 2 (dimensionless time-scale units) is used, but if readers find it clearer to assign real times to the time-step values, then it would be appropriate to assume, as a first indication, that one time step equals 500 yr (assuming an initial erosion rate of 10^{-5} times the initial ice thickness; for example, 1 mm/yr under an initially 100-m-thick glacier), as long as they are aware of the problems inherent in attaching absolute times to the simulation results. Although empirical estimates of glacial erosion rates vary over two orders of magnitude (Drewry, 1986), Humphrey (1987) has shown that when erosion rates are scaled relative to ice velocity, the level of variation is a factor of two to three, and thus time-scale estimates for form evolution are probably no more accurate than this level.

Ice Discharge Constraints

In the simulations described here, it is assumed initially that ice discharge through the cross section remains fixed over time, thus the initial form development results are valid primarily for situations in which ice discharge is truly time invariant or situations in which form development is controlled by conditions at some dominant ice discharge. In later simulations, it is assumed that ice discharge varies cyclically, with a period of 100 ka; however, an ice discharge constraint of some sort (either temporally uniform or nonuniform) is crucial in controlling large-scale form development. If ice discharge is not prescribed, and the ice surface remains at some fixed elevation (the implicit assumption of many semi-quantitative analyses of cross-section development; for example, Johnson, 1970; Boulton, 1974), then as cross-section area and ice thickness increase because of the effects of erosion, ice discharge also increases extremely rapidly. Discharge through a section scales approximately with centerline depth to the fifth power (Paterson, 1981); thus a tripling of ice thickness will increase ice discharge 243-fold. Although such increases in ice discharge may not be totally unreasonable for some time periods, it is more reasonable to control ice discharge explicitly than to keep the ice surface elevation fixed and implicitly assume that ice discharge increases as an extremely sensitive function of the erosion rate.

Model Output and Measures of Form Development

At each time step, the model calculates the form of the cross section as a series of coordinates for the glacial channel and valley walls. Analysis of general development trends and comparison of model predictions with empirical data require some measure of profile form. Much of the existing morphometric work on glaciated valleys has involved fitting a power law equation, of the form

$$z = ay^b \tag{3}$$

to empirical data for bedrock profiles, where y and z are horizontal and vertical distances from the section low point respectively, and a and b are constants, determined by a least-squares fit to a logarithmic transformation of the section coordinates (Svennson, 1959; Graf, 1970; Doornkamp and King, 1971; King, 1974; Aniya and Welch, 1981; Wheeler, 1984; Aniya and Naruse, 1985; Hirano and Aniya, 1988). With standard methodology, the power-law coefficients primarily reflect the form of the lower part of the cross section (Harbor and Wheeler, 1992), which is the part of the profile most likely to be representative of the most recent active glacial channel.

It is commonly argued that cross-profile morphologies progress from a V-shape to a U-shape under prolonged glacial erosion, and, in this case, one might hypothesize that b values for glaciated valleys change systematically from values close to 1.0 (V-shaped, little glacial modification) to values close to 2.0 (U-shaped, glacial modification dominates the form) (for example, King, 1974; and discussed in Harbor, 1990b, and Hirano and Aniya, 1990). For this reason, much of the empirical work has consisted of determining b values for glaciated valleys. The power function (equation 3), however, describes an endless curve, thus a complete description of the valley geometry also requires a description of the part of the curve being used (Graf, 1970). Defining a form ratio (FR) as

$$FR = \frac{D_v}{W} \tag{4}$$

(Graf, 1970) where D_v is the valley depth and W is the valley top width, sections only appear similar in form if they have closely matched a values, b values, and form ratios (Fig. 4).

The aim of providing some measure of form development as a part of the model procedure is to allow both for the tracking of progressive form development during simulation runs and for comparison of the model results with empirical data. Form development is described in the model in terms of b and FR values for the active glacial channel and the glacial valley, and this allows for consistent comparison both within and between simulations. There is some difficulty in interpreting correspondence or lack of correspondence between the model predictions and the empirical results, however, because of problems in accurately deriving these types of values for glaciated valleys (Harbor and Wheeler, 1992). Despite this, such comparisons are highly desirable as they provide the most reasonable initial check on model predictions.

INITIAL MODEL RESULTS

The first application of the model examines cross-section development under conditions of uniform ice discharge and spatially uniform bedrock resistance to erosion. This simulation of the simplest initial conditions is important because it provides clear insight into the way that glacial-valley cross sections can develop solely as a consequence of glacial erosion. Building on this, subsequent simulations are used to assess the sensitivity of the simulation results to variations in ev, the basal velocity exponent in the erosion law, which allows examination of the ability of

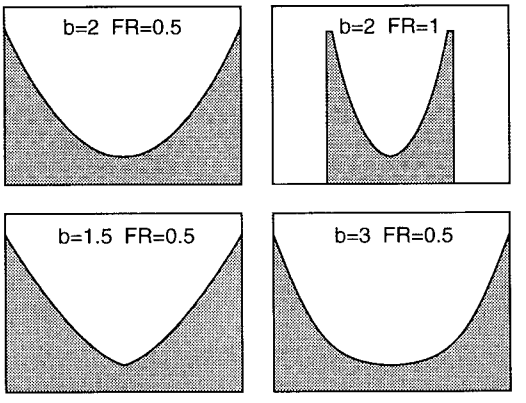

Figure 4. Form differences for cross sections with varying *b* and *FR* values. The upper two sections have identical *b* values but different form ratios, whereas the lower sections have identical form ratios but different *b* values.

landform modeling to test alternate forms of the erosion law in terms of their capacity to predict the development of a well-known glacial landform. Simulations of form development under more complex conditions of temporally variable ice discharge are described in a subsequent section.

Initial Development

The initial condition for the first simulation is a V-shaped active glacial channel ($b = 1.0$), with $FR = 0.5$, $ev = 2$ and the relative time-scale option. The velocity solution for the initial cross section includes marked lateral variations in basal sliding velocities (Fig. 5). Sliding velocities at the margin of the active glacial channel are only 18.2% of the maximum basal velocity and are low because of the retarding influence of high effective pressures near the margin where the piezometric surface intersects the bed (Fig. 3). Basal velocities increase toward the center of the glacier as the ice thickness increases and the effective pressure decreases (Fig. 3), but increased drag associated with the constricted form right at the center of the V-shaped channel reduces velocities in this area to give a central minimum in the basal velocity distribution (Fig. 5). With an erosion law dependent primarily on basal velocity, this marked spatial variation in basal sliding yields an erosion pattern with maxima somewhat removed from the center of the channel and minimum erosion at the glacier margins. As McGee (1894), Matthes (1930), and Johnson (1970) realized from simple geometric constraints, this is precisely the erosion pattern required to convert a V-shaped to a U-shaped active glacial channel. Higher erosion rates away from the center progressively reduce the elevation difference between the center and adjacent areas, effectively removing the central constriction of the initial V-shaped active glacial channel. With this change in form, there are corresponding changes in flow and erosion patterns, because without a central constriction retarding flow, the maximum velocity is at the center of the channel. As the constriction is progressively removed, the points of maximum basal velocity and erosion move toward the center of the section, eventually eliminating the local minima in erosion and velocity to give a concave-upward form (Fig. 5). There are also significant changes in basal velocities toward the glacier margins: as the active glacial-channel walls become more concave, the lateral slope of the bed near the margins is increased, and this results in a progressive increase in marginal sliding velocities.

Effects of the Ice-Discharge Constraint

In the first few time steps, the consequences of the constant ice-discharge constraint become clear. Each time the coordinates of the active glacial channel are altered to account for erosion, the cross-sectional area of the glacier is increased, and the shape of the active glacial channel is modified. These changes would cause an increase in the ice discharge through the section if the ice-surface elevation were held constant for the next time step. To control this, the model procedure lowers the ice surface after each erosion iteration to a position that yields a discharge equal to the discharge through the initial section. Because the active glacial-channel walls slope toward the center of the glacier, any lowering of the surface also effectively narrows the active glacial channel, and it is the balance between this narrowing and lateral erosion at the margin that dictates the net change in the width of the active glacial channel for each time step. During the initial period of rapid form evolution, narrowing dominates, producing a progressive decrease in active glacial-channel width as the glacier incises the landscape. As the form evolves, however, marginal velocities (and thus marginal erosion rates) increase, and the drop in surface elevation per time step required to maintain constant ice discharge decreases, and thus the difference between the narrowing and widening

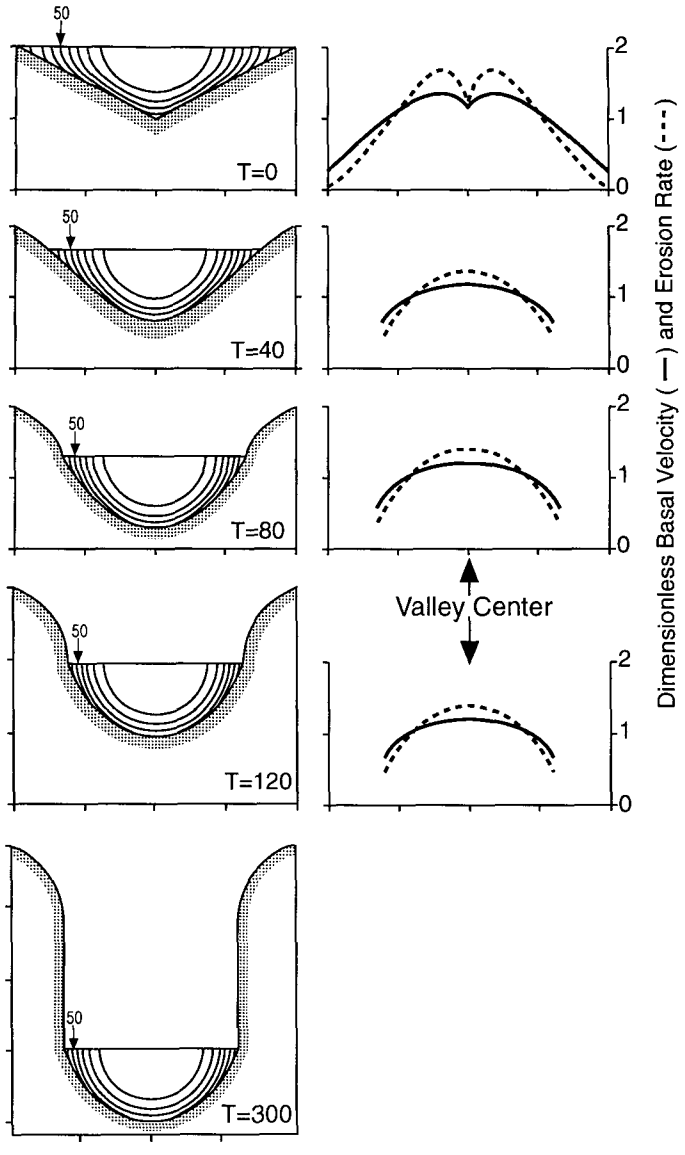

Figure 5. Model results for a simulation of form development with erosion scaled to the local basal velocity squared. The figures show the glacial-valley cross section at different time steps (T), with velocity contours on the glacier in units of 10% of the maximum velocity for the section, and with the most central contour being 90%. The plots are dimensionless and are shown with no vertical exaggeration. The graphs show corresponding cross-glacier variations in basal velocities and erosion rates, in each case scaled to an average cross-section value of one. The basal-velocity and erosion-rate distribution for T = 300 (not shown) is essentially identical to that for T = 120.

effects are progressively reduced. This trend of declining narrowing rates, combined with continued vertical incision, leaves behind convex valley slopes in the zone of glacial influence above the active glacial channel (Fig. 5). It is important to note that these "glaciated shoulder" forms (Cotton, 1941) are developed not because of slope processes (which are ignored here) but simply because of the interaction between the subglacial erosion pattern and ice-surface lowering, commensurate with overall glacial incision.

The Steady-State Form

Expressing the development of the active-channel form in terms of b and FR values, after a period of relatively rapid initial form change, the active glacial channel eventually reaches a steady-state configuration (Fig. 6). Although true steady state (no subsequent change in b or FR values) is reached at time step 194, by time step 112 the active glacial channel b value has undergone 95% of the change involved in reaching the steady-state form (Fig. 6). At steady state, the basal velocity and erosion distributions consist of a simple maximum at the center of the active glacial channel, with bed-normal erosion rates and velocities at the glacier margin of 31% and 56%, respectively, of the rates found at the center of the channel (Fig. 5). This steady state for the active glacial channel is reached when the combination of the cross-sectional pattern of bed-normal erosion and the effect of surface lowering produce a net erosion at all points on the cross section that is equivalent to uniform lowering (that is, perfect form translation). It is important to note that this type of steady state arises primarily because of the ice-discharge constraint. In the absence of such a constraint, one could also conceive of a steady state in which bed-normal erosion was everywhere equal, but such a situation would be problematic for two main reasons: first, it would require equal basal velocities at all points on the bed if a purely velocity-dependent erosion law were used (in marked contrast to the empirical evidence for significant lateral variations in sliding velocities); and, second, to maintain such a form would require a continuous and very rapid increase in cross-section area and thus ice discharge (because discharge scales approximately to the fifth power of ice depth, Paterson, 1981), which could not be sustained for long periods of time.

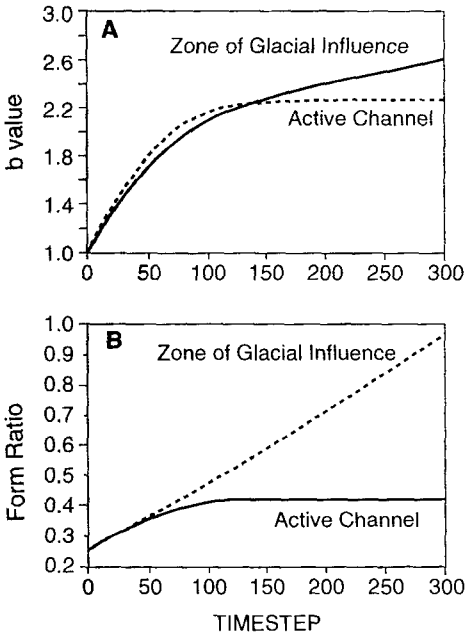

Figure 6. Form development as indicated by changes in b and FR values for the active glacial channel and the zone of glacial influence. In this simulation, erosion is scaled to the local basal velocity squared, and ice discharge through the section is held constant. Note that after an initial period of rapid form development, by time step 194 a steady-state active glacial channel has evolved. Subsequent to this, the active glacial channel continues to incise vertically but does not change form.

At time step 194, when the steady state is reached, the form of the cross section is characterized by b = 2.26 and FR = 0.41 for the active glacial channel, and b = 2.39 and FR = 0.70 for the zone of glacial influence. At time step 112 (95% of active-channel form change has occurred), b = 2.20 and FR = 0.40 for the active glacial channel, and b = 2.13 and FR = 0.50 for the zone of glacial influence. Empirical studies of glaciated valleys (representative primarily of zones of glacial influence) typically give values in the range b = 1.5 to b = 2.4 and FR = 0.1 to FR = 0.6 (most of the data are summarized in Hirano and Aniya, 1988); thus the simulation predictions are consistent with the empirical data, even though the empirical data represent valleys which have been subject to differing degrees of glacial erosion. Although there is as yet little published data for b and FR values for active glacial channels against which to compare the model predictions, the model predictions for the active glacial channel steady-state form are consistent with sections of the Variegated Glacier and Athabasca Glacier described by Bindschadler and others (1977) and Raymond (1971), which have b values in the range b = 1.2 to b = 2.4 and form ratios between FR = 0.15 and FR = 0.55 (Fig. 7).

Further Development of the Glacial Valley

The steady-state form for the active glacial channel is reached at time step 194, and, in subsequent time steps, this active glacial channel form is simply translated vertically. The glacial-valley form, however, continues to change beyond time step 194 because vertical incision of the active glacial channel increases the length of vertical slope elements left above the glacier. Under sustained erosion, this results in a valley form dominated by vertical side walls, above which there are small convex slope sections (Fig. 5). This arises in the absence of any consideration of slope processes and matches the general form of many deeply incised glaciated valleys (see, for example, sections of the Yosemite Valley *in* Matthes, 1930). This unchecked deepening of the valley, which eventually increases the b and FR values for the zone of glacial influence well beyond the range of the

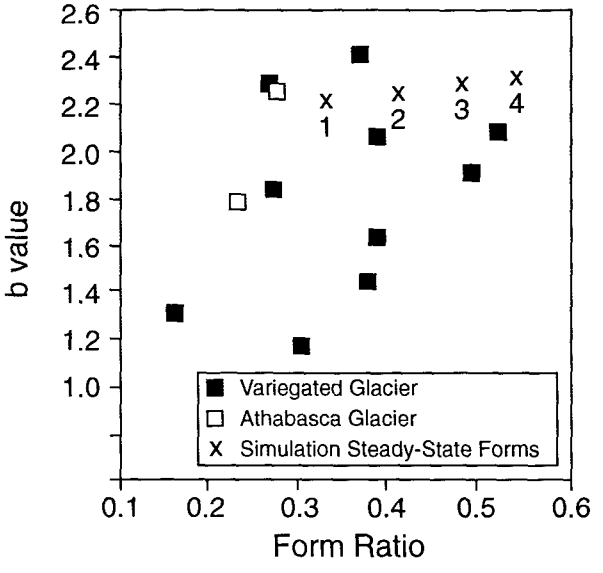

Figure 7. Diagram plots b and FR for sections of the Athabasca and Variegated Glaciers, based on profiles from Raymond (1971) and Bindschadler and others (1977). The model predictions for the steady-state active glacial channels (ev values of 1 to 4 shown) fall generally within the range of the empirical data.

empirical data (particularly for *FR*, Fig. 6), does, however, highlight an important limitation in one aspect of the current model. By maintaining constant ice discharge, the model fails to account for potential reductions in discharge as the section erodes to lower elevation levels where, all other things being equal, one would expect lower mass balances and thus lower ice discharges. If the model were structured to give progressively lower discharges below some equilibrium-line elevation, then, with the current erosion model, the rate of vertical incision would decrease as the active glacial channel eroded to lower elevations, approaching a condition of zero erosion at the terminus elevation. In some areas, sea level would also provide an effective base-level control on the vertical component of erosion. Thus, the accuracy of simulation predictions for form development associated with very extensive vertical erosion is limited by the lack of effective feedback mechanisms to reduce ice discharge and/or erosion rates at lower elevations.

Sensitivity of Form Evolution to Variations in the Erosion Exponent

To assess the sensitivity of the model results to variations in the value of the velocity exponent in the erosion law, simulations were run with exponent values (*ev*) ranging from 1 to 4. Although there is no theoretical justification for such a range of values, the analysis allows an assessment of the extent to which form evolution might provide constraints on potential forms of the erosion law. As well as improving our understanding of form development, numerical landform development models offer the opportunity to test potential erosion laws in terms of their ability to predict the development of known landforms.

For $ev = 1.0$, although no true steady state was reached by run termination (Fig. 8), the b value for the active glacial channel was increasing slowly at $b = 2.22$ with a form ratio of $FR = 0.33$. For $ev = 2.0$, as has already been discussed, a steady state with $b = 2.26$ and $FR = 0.41$ was reached after time step 194. For larger values of *ev*, steady-state conditions are reached at slightly earlier time steps and consist of progressively higher b and *FR* values (Table 1). The most striking aspect of these results is that with increasing values of *ev* the active glacial channel becomes narrower and deeper, for a given ice discharge (Fig. 9).

As empirical studies provide b and *FR* values consistent with the entire range of *ev* values considered here, these results do not clearly rule out any possible values of *ev*. Empirically derived b values, however, are typically in the lower range of the values given in Table 1, and thus there is some suggestion that *ev* values of 1.0 to 2.0 produce results more in accord with the empirical observations than higher values of *ev*. This also agrees with Hallet's (1979, 1981) theoretical work on abrasion which suggests that abrasion rates scale approximately with basal velocities raised to a power of one to two.

Initial Results: Discussion and Conclusions

With an assumption of constant ice discharge, and scaling the erosion rate to local basal velocity squared, the simulation model predicts form evolution dominated by vertical incision and a progressive transformation of the active glacial channel from an initial V-shape to a steady-state, quasi-parabolic form. The form of the steady-state active glacial channel and that of the zone of glacial influence (at the time that steady state is reached for the active glacial channel) agree well with empirical observations. As the glacier incises vertically, the ice surface is lowered (to maintain constant ice discharge), and as marginal erosion rates are initially low, the active glacial channel is progressively narrowed. As marginal erosion rates and side-slope angles increase, however, narrowing decreases, and the net effect of this change during overall vertical incision is to leave slopes, above the glacier, consisting of a convex valley shoulder in the upper regions of the zone of glacial influence, above vertical walls.

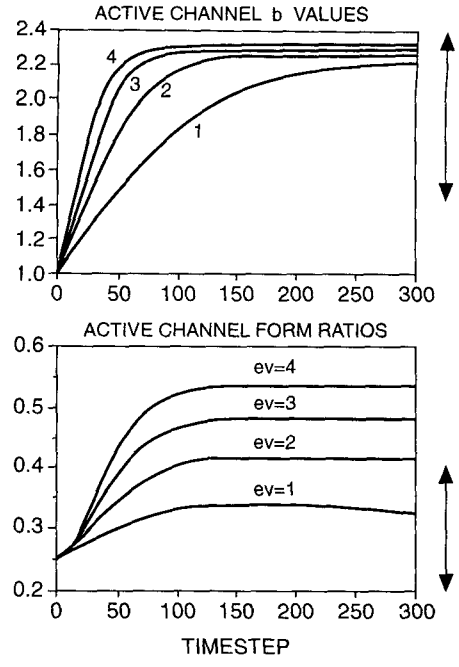

Figure 8. Comparison of form development with different values of *ev*, the exponent for velocity in the erosion law, as indicated by changes in active glacial channel *b* values and form ratios. Although in all of these cases a broadly parabolic, steady-state active glacial channel was developed, these represent quite a range of forms, as there is considerable variation in form ratios (see Fig. 9). The arrows on the plots indicate the range of values for empirical data given in Figure 7.

Although the model predictions with an erosion law that scales erosion rates with basal velocity squared match the general characteristics of the empirical data, with exponent values between one and four the general pattern of form evolution is similar, with eventual development of a steady-state, quasi-parabolic active glacial channel below side slopes with an upper convex element above vertical sidewalls. There are, however, variations in active glacial channel form, in particular form ratios, with higher exponent values giving larger form ratios (relatively narrower, deeper cross-section forms). Although empirical studies provide form-ratio values consistent with the entire range of exponent values, there is some suggestion that exponent values of one and two produce results more in accord with the majority of the empirical data than do higher exponent values.

TABLE 1. VARIATIONS IN STEADY-STATE CHANNEL FORM AS A FUNCTION OF THE EROSION EXPONENT (*ev*)

ev	*b*	*FR*
1	2.22	0.33
2	2.26	0.41
3	2.29	0.48
4	2.32	0.54

Note: b is the exponent in the power-law fit to the cross section, and *FR* is the form ratio of the section. The b value for $ev = 1$ was still increasing slowly at the end of the simulation and so does not represent a true steady state.

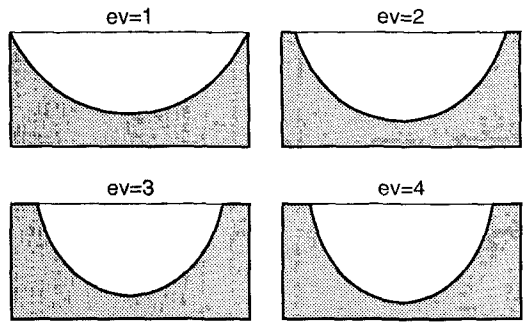

Figure 9. Comparison of steady-state, active glacial-channel forms for four values of *ev*, the velocity exponent in the erosion law. Narrower, deeper, active glacial channels are developed when values of *ev* increase.

The time scale for form evolution is also of considerable interest, but it is sensitively dependent on some initial assumption for absolute erosion rates. As data from present-day glaciers provide glacial erosion rates, scaled to ice velocities, that vary over a factor of two to three (Humphrey, 1987), predicted time scales will vary over a similar range. With an initial erosion rate 10^{-5} times the initial ice thickness (for example, 1 mm/yr under an initially 100-m-thick glacier), the b value for the active glacial channel is at 95% of the steady-state value after ~56 ka, and a b value at the low end of the range of the empirical data is reached after only on the order of 15 ka of sustained erosion. Although somewhat speculative, this order of time scale suggests that where erosion rates are high, recognizably "glacial" valleys can be developed during a single glaciation, whereas where erosion rates are low, several glaciations would be required to produce such a form. This rapid form development may explain why U-shaped valleys are one of the most widely recognized features of alpine glacial landscapes.

MODEL RESULTS: FORM EVOLUTION WITH TEMPORAL VARIATIONS IN ICE DISCHARGE

In the simulations presented so far, it has been assumed that glacial valleys develop under conditions of constant ice discharge. It is well known, however, that during the Quaternary there have been significant climatic changes over a range of temporal and spatial scales. These changes had major impacts on glacier mass balances, leading to the expansion and contraction of both alpine and continental ice masses, and were largely responsible for the present occurrence of glacial landforms well beyond current glacial limits. It is clearly important to attempt to assess how important temporal variations in ice discharge might be for form evolution. Would forms evolve under conditions of varying ice discharge that are similar to those predicted for the constant-ice-discharge case, and how important are temporal variations in ice discharge in controlling the net erosion pattern across a glacial valley? These are questions that have been addressed rarely in past work, and yet they seem crucial if detailed process models are to be used to predict landform evolution.

Temporal Variations in Ice Discharge

The model procedure allows for a wide range of possible forms for temporal variations in ice discharge, but a single example is sufficient to indicate the main characteristics of form evolution under these types of conditions. The deep-sea oxygen-isotope record provides a record of global-scale variations in ice discharge (Emiliani, 1955; Shackleton and Opdyke, 1973) and, although there clearly may be considerable departures in the discharge records of individual glaciers from this global average, it seems reasonable to suggest a broadly similar trend for the purposes of modeling general landform evolution. Thus, in this illustration of form evolution under varying ice discharge, I use a discharge record consisting of five 100-ka cycles, with each cycle consisting of a simple monotonic increase in ice discharge from a minimum value to a maximum value over 80 ka, followed by 10 ka at the maximum ice discharge, and a final 10 ka during which ice discharge decreases monotonically again to the minimum value at 100 ka. This embodies the essence of characteristic variations in global ice volume as reflected in the marine isotope record: a relatively slow buildup of ice followed by an abrupt reduction in ice volume.

As an initial analysis of the effects of temporal variations in ice discharge, I consider a case in which a V-shaped valley with an initial active glacial channel depth of 300 m and a half-width of 600 m is subject to five 100-ka cycles of glacial erosion. During each cycle, ice discharge through the section varies temporally, with the maximum ice discharge set at that which would occur in a V-shaped active glacial channel with a depth of 900 m and a half width of 1,800 m. Additionally, I assume $E = 10^{-4}\ U_b$, (Humphrey, 1987) in an attempt to scale absolute erosion rates appropriately to sliding velocities that vary with ice discharge.

Glaciological Constraints

For simulations with large-scale variations in discharge, and thus ice thickness, certain assumptions made for the constant ice-discharge case are no longer appropriate. In particular, with variable ice discharge, it is necessary to allow for variations in the ice-surface angle and the relative position of the piezometric surface. Modeling significant variations in ice discharge at one cross section is somewhat analogous to modeling different sections along the length of a single glacier at one point in time, and, for this case, it is known that there are variations in surface angle and the relative position of the piezometric surface (Röthlisberger, 1972; Hodge, 1974; Bindschadler and others, 1977; Bindschadler, 1983). These are important variables in the analysis because the surface angle affects both deformation rates and sliding velocities through its impact on shear stresses, and the position of the piezometric surface controls effective pressures which are an important component of the sliding velocity calculations.

In the model runs with variable ice discharge, the surface angle is constrained by imposing the requirement that the centerline basal shear stress varies between 0.8 bar (low-discharge case) and 1.2 bar (high-discharge case). Although this is a somewhat arbitrary way of treating basal shear-stress variations, laboratory and field data suggest that values of the basal shear stress should range between 0.5 bar and 1.5 bar (Pierce, 1979; Paterson, 1981), and measurements on current and reconstructed glaciers suggest that away from the terminus basal shear stresses increase with increasing ice thickness, with values given in Bindschadler (1983) and Murray and Locke (1989) providing the basis for the estimated range of τ_b = 0.8 bar to τ_b = 1.2 bar used here. As the simulations include an approximate three-fold increase in ice thickness, but only a 50% increase in τ_b, surface-slope angles are necessarily reduced with greater ice thickness. This slows the rates of increase in both internal deformation and basal sliding with increasing ice thickness, compared to a situation in which the surface angle is held constant.

For variations in the piezometric surface position with changing ice thickness, it is assumed that the piezometric surface remains a fixed distance below the ice surface. This accords with the theoretical results of Röthlisberger (1972) and Bindschadler (1983), and the empirical data of

Hodge (1974), which show that in the longitudinal direction for individual glaciers, regardless of bed topography, the piezometric surface remains at approximately a uniform distance below the ice surface. In the modeling, the effect of this requirement is to give decreased effective pressures with increased ice thickness, and, as the sliding velocity scales inversely with effective pressure, this gives greater sliding velocities under thicker glaciers.

Results

In this analysis of the effects of variations in ice discharge on form evolution, the initial condition (Fig. 10) is marked by erosion and velocity distributions with a local central minimum superimposed on a general pattern of increasing basal velocities and erosion rates toward the center of the glacier. For this low-discharge case, basal velocities are relatively small (3.8–11.5 m/yr) because the piezometric surface is low, and thus effective pressures are relatively high. With increasing ice discharge, there is a rapid increase in ice depths, basal velocities, and erosion rates, and, as the glacier is more extensive laterally, erosion affects a larger portion of the valley cross section. By 50 ka basal velocities have risen to 4.4–47.6 m/yr, giving a three-fold increase in erosion rates compared to the low-discharge condition, and by 90 ka, the maximum-discharge condition, basal velocities have risen to 5.8–73.3 m/yr, giving a four-fold increase in erosion rates compared to the low-discharge condition (Fig. 10). As the ice level falls toward the end of the first cycle, velocities decrease, and the glacier occupies a progressively smaller portion of what was the active glacial channel at the maximum ice extent (Fig. 10). With low velocities and a smaller total extent, little form development occurs toward the end of the glacial cycle. Expressing form evolution in terms of b and FR values for the active glacial channel, much of the change in form occurs in response to the high-discharge phase of the glacial cycle (the active glacial-channel form is in a state of flux, but its form only approaches equilibrium with the flow dynamics in the terminal phase of slow ice buildup, Fig. 11). By the end of the first 100-ka cycle, the active glacial channel has b = 1.75 and FR = 0.25. During the second erosion cycle, b values continue to increase, and, by the end of the second cycle, b values are between 2.0 and 2.5, and they remain in the range 2.2 to 2.4 during all subsequent cycles. Within this range, maximum b values correspond to periods of maximum ice discharge and are approximately constant for each successive cycle, indicating that a dynamic steady-state form has effectively been reached. Active glacial-channel form ratios show much wider variation. At high ice discharges, the form ratio is high (FR = 0.6), a relatively deep, narrow channel, but form ratios decrease at low discharges (FR = 0.2) because the glacier occupies the low-gradient section of what was the center of the high-discharge active glacial channel. This major change in the active glacial-channel form ratio reflects a decrease in ice elevation rather than any significant change in the form of the glacial valley.

Overall profile development for the first four 100-ka cycles of erosion is shown in Figures 10 and 12. By 390 ka the glacier is at a maximum discharge state and has central sliding velocities as much as 80 m/yr and local erosion rates as much as 8 mm/yr (Fig. 12). The progressive development of the valley, shown in Figure 12, emphasizes the fact that in a sequence of glacial cycles, even though maximum ice discharges may be identical, maximum ice elevations attained vary markedly through time because of the progressive downcutting of the glacier. The maximum ice elevation for the first cycle is 1.5 km higher than that for the fourth cycle, even though in both cases the maximum ice discharge was the same. Although this is an extreme example, it does indicate the general point that when attempting to reconstruct paleoglaciers it is important to consider the possible extent of valley modification since the time of interest, because this can have substantial impacts on estimates of paleo discharge and thus paleoclimatic conditions. In the simulation results, the maximum ice levels of successive cycles stand out prominently as breaks in slope and overhangs (Fig. 12), which developed because of the contrast between lateral erosion at the maximum ice margin and the lack of erosion above the maximum ice surface. If the model also accounted for significant subaerial slope processes, the overhangs would collapse in some cases; nonetheless, this pattern of slope-profile changes related to successive cycles matches previous explanations of benches or shoulders in glaciated valleys as "preserving relics of the troughs of successive glaciations" (Cotton, 1941, p. 92).

The simulation model also predicts the temporal variation in cross-sectionally averaged erosion rates and sediment output from the section, assuming that there is no significant change in sediment storage over the time scale considered here (Fig. 13). Although the absolute values

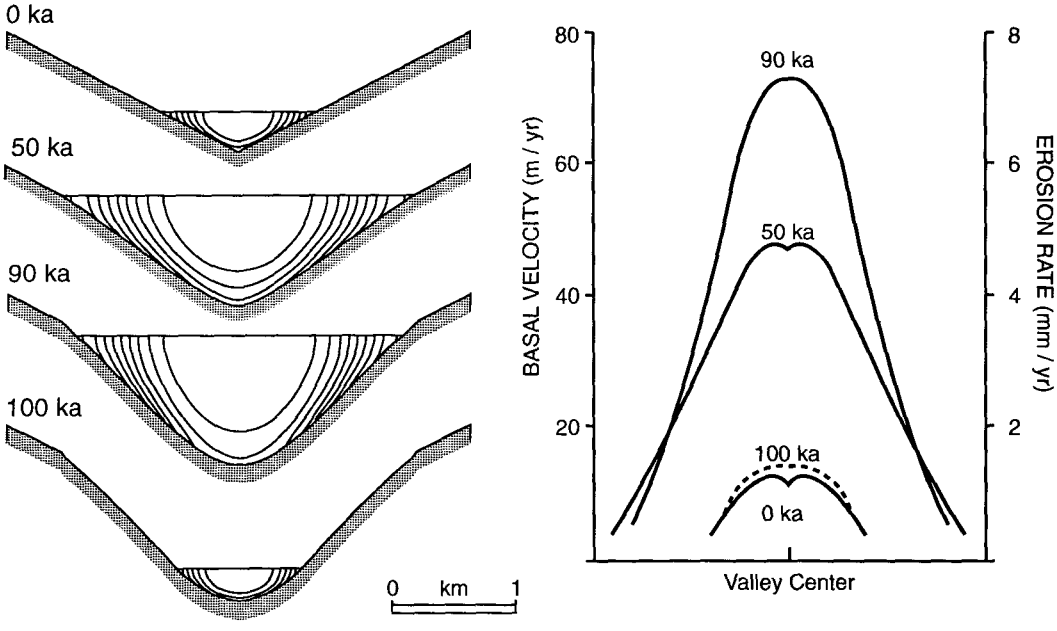

Figure 10. A simulation of cross-section form development over an idealized 100,000-yr glacial cycle with temporally varying ice discharge. Velocity contours for the glacier sections are in units of 10% of the maximum velocity for the section, with the central contour in each case at 90%. The graph shows changes in patterns of basal velocities and erosion rates for the section. Note that because erosion is scaled linearly with velocity in this simulation, the erosion and velocity profiles plot as a single line on the graphs.

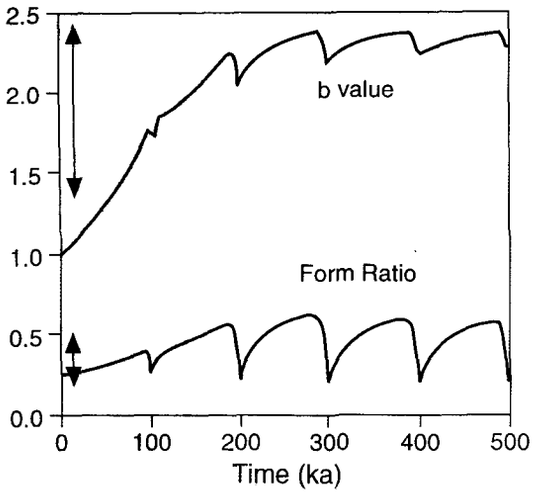

Figure 11. Diagram for active-channel form evolution, showing *b* and *FR* values plotted over five 100,000-yr glacial cycles with temporally varying ice discharge. The arrows on the plot indicate the typical range of values for the empirical data.

length, and the minimum sediment production is equivalent to 1.5×10^4 m^3/yr (3.75×10^7 kg/yr). For comparison, empirical data from present-day glaciers give typical erosion rates on the order of 0.1 to 5.0 mm/yr and sediment output rates on the order of 10^6 to 10^8 kg/yr (data summarized in Drewry, 1986). Considering that present-day glaciers are typically at the low-discharge phase of a glacial cycle, and that predicted low-discharge average erosion rates and sediment outputs are in the middle of the range of empirical values, there is at least an order of magnitude agreement between the empirical data and the model results.

Discussion and Conclusions: Variable-Discharge Simulations

The predicted development of cross-section form under conditions of temporally varying ice discharge departs somewhat from predictions made using an assumption of constant ice discharge. With variable ice discharge, the model predicts a range of *b* and *FR* values, depending on ice discharge, and the steady-state values for constant discharge are close to this range (Table 2). Thus, although it is clear that under varying ice discharge form evolution is strongly affected by high-discharge conditions (when erosion rates are highest, and the glacier is most extensive laterally), the degree of convergence in form evolution with the constant-discharge case is depend-

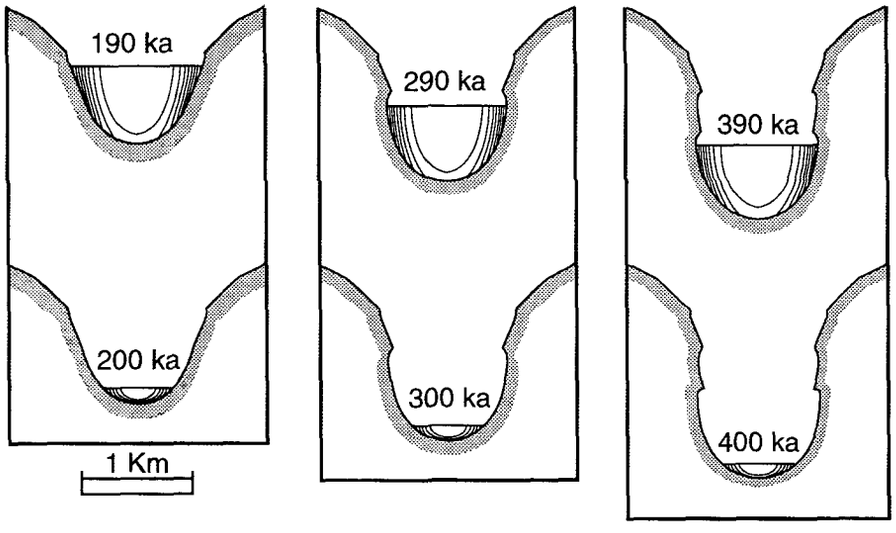

Figure 12. Cross-section form development with temporally varying ice discharge, glacial cycles 2 to 4. In each case, the upper figure shows conditions at maximum ice discharge for the cycle, and the lower figure shows minimum-discharge conditions. Velocity contours for the glacier sections are in units of 10% of the maximum velocity for the section, and in each case, the most central contour is 90%.

are subject to considerable uncertainty (as they are directly dependent on the assumed scaling between basal velocity and erosion rates), the general pattern is instructive, considering recent discussions of the relationship between glacial cycles and changing denudation rates (Molnar and England, 1990, 1992; Summerfield and Kirkbride, 1992; Harbor and Warburton, 1992). Erosion rates follow the discharge trend closely, and, in this simulation, maximum cross-sectionally averaged erosion rates (5 mm/yr) are five times the minimum (low-discharge) values. This is probably a rather conservative estimate of the erosion difference between low-discharge and high-discharge glaciers, because maximum velocities in this simulation are low compared to present-day fast-sliding glaciers, such as ice streams and surging glaciers. The difference in average erosion rates is amplified in the sediment-production trend as the higher erosion rates occur during periods when the glacier is more extensive laterally, thus erosion is not only faster but affects a larger area. The maximum sediment production rate of 14 $m^3/m/yr$ corresponds to a total sediment output of 1.4×10^5 m^3/yr (3.5×10^8 kg/yr), assuming that the glacier is 10 km in

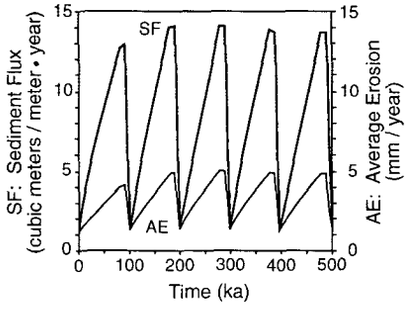

Figure 13. Variations in total sediment output and cross-sectionally averaged erosion rates under conditions of temporally varying ice discharge (five idealized 100,000-yr glacial cycles).

TABLE 2. ACTIVE GLACIAL-CHANNEL *b* AND *FR* VALUES FOR THE CONSTANT AND VARIABLE DISCHARGE SIMULATIONS

Active glacial channel	Constant ice-discharge case	Variable ice-discharge case	
		Maximum discharge	Minimum discharge
b	2.23	2.37	2.28
FR	0.43	0.58	0.20

Note: values for the variable-discharge cases are taken from 490 ka (maximum discharge) and 500 ka (minimum discharge).

ent on the relative amount of time spent at, or close to, high-discharge conditions.

The most striking aspect of the difference between the constant-discharge and variable-discharge results is the change in form ratios, with the variable-discharge case giving much higher maximum discharge form ratios (relatively deeper and narrower active glacial channels) than the constant-discharge case. This arises because form ratios are sensitively dependent on the ratio between lateral and vertical erosion rates. With varying ice discharge, and thus ice extent, although the center of the zone of glacial influence for any given cycle is subject to erosion throughout the cycle, the marginal areas at high discharges are subject to erosion for only a small portion of the cycle. Thus for the variable-discharge case, erosion is enhanced at the center of the zone of glacial influence. It is this difference in the relative scaling of lateral and vertical erosion rates that accounts for the difference in form ratios between the constant- and variable-discharge simulations.

There is also a significant difference between the form of the active glacial channel at low-discharge states compared to predictions based on constant discharge (Table 2). In particular, form ratios are much lower in the variable-discharge case, because these low-discharge forms are largely inherited from the effects of erosion at high-discharge conditions. In essence, the low-discharge glaciers are "underfit," to borrow a term from fluvial geomorphology. This is an important point because it means that for present-day glaciers, which are typically in the low-discharge state of the current interglacial, one should not expect a good correspondence between current erosion patterns and present active-glacial channel form. Thus, for modeling active glacial-channel development, ice-discharge variations are crucial. This also explains why predictions of active glacial-channel form, made assuming constant ice discharge, do not match the form characteristics of present-day glacier sections (in particular, form ratios) and implies that, if form evolution is to be used to provide an indication of the most appropriate values of the sliding-law exponents, it is necessary to use variable-discharge simulations.

Another interesting aspect of the variable-discharge results is the prediction that during the first two glacial cycles *b* values increased progressively from an initial value of $b = 1.0$ to $b = 2.5$ (Fig. 11). To a first approximation, this increase is linear with time, lending support to the contention that, under sustained erosion, *b* values increase progressively, representing a transformation from an initial V-shaped active glacial channel to a quasi-parabolic form (King, 1974). Thus *b* values provide a relative measure for the degree of glacial modification and the relative time period of glacial erosion, if the initial form of the active glacial channel is known, and there are no significant lithological variations between sites (Augustinus, 1992). For $b > 2.0$, however, there is no consistent pattern of increasing *b* values with time, and thus *b* values no longer provide a relative measure of the time period of glacial erosion. There are at least two additional complications. First, it is generally difficult to estimate the preglacial form, unless there are areas above the subsequent zone of glacial modification that remain largely unchanged to allow extrapolation of form into the area subsequently modified by glacial action (Matthes, 1930). Even if this is the case, predicted preglacial profiles vary significantly depending on the assumptions made regarding the long-profile form of preglacial drainages (see Harbor, 1989). Second, in the model no account is taken of the climatological feedbacks associated with extensive vertical erosion. During a period of 500 ka, the cross section is lowered in excess of 2.5 km and, unless this was counteracted by rapid uplift, this would shift the glacier section to much lower elevations where one would expect far lower ice discharges for any given stage of the glacial cycle (see, for example, modeling of glacier long-profile development *in* Oerlemans, 1984). One could predict, therefore, a negative feedback developing where vertical erosion reduces ice discharges, which would in turn reduce erosion rates. In addition, in certain areas, erosion would lower the section progressively to sea level, at which time basal water pressures might rise initially, giving high sliding velocities and erosion rates, until the glacier became uncoupled from its bed (flotation) and erosion ceased.

FUTURE WORK

Although the work presented here advances our understanding of the nature and rate of valley cross-section development by glacial erosion, a major limitation of the current model is that it cannot address the complications that arise from the fact that glacier cross sections are not isolated entities, but part of three-dimensional systems. Thus the model ignores important feedbacks which may arise with respect to long-profile variations in form and glaciological and climatological conditions. Clearly, the problem of glacial-valley development would best be addressed using a three-dimensional model of glacier flow to examine the interactions between long- and cross-profile development, but a glaciological model on which to base this is not available as yet. Two-dimensional models for the long-profile flow problem are available, however, and could be productively applied to examine the development of long-profile forms, in particular overdeepenings.

The other primary limitation of the model is the lack of consideration of extra-glacial slope evolution. Models of such processes (for example, Augustinus, 1988, 1992), however, could be combined fruitfully with the glacial model to examine the interaction between glacial and hillslope processes in the development of glaciated-valley forms.

ACKNOWLEDGMENTS

This work would not have been possible without the guidance and support of Bernard Hallet, Charlie Raymond, Steve Porter, Tom Dunne, and Ed Waddington at the University of Washington. I am also grateful to W. Harrison and an anonymous reviewer for their helpful comments on this paper. Funding for this work was provided by National Science Foundation Grant EAR-8708400 (to Bernard Hallet) and a fellowship from the Shell Companies Foundation. Additional support for completion of this paper was provided by the Department of Geology, Kent State University.

REFERENCES CITED

Aniya, M., and Naruse, R., 1985, Structure and morphology of the Solar Glacier, *in* Nakajima, C., ed., Glaciological studies in Patagonia Northern Icefield, 1983–1984: Data Center for Glacier Research, Japanese Society of Snow and Ice, p. 70–79.

Aniya, M., and Welch, R., 1981, Morphological analyses of glacial valleys and estimates of sediment thickness on the valley floor: Victoria Valley system, Antarctica: The Antarctic Record, v. 71, p. 76–95.

Augustinus, P. C., 1988, The influence of the lithological and geotechnical properties of rocks on the morphology of glacial valleys [Ph.D. thesis]: Hamilton, New Zealand, University of Waikato, 257 p.

Augustinus, P. C., 1992, The influence of rock mass strength on glacial valley cross-profile morphometry: A case study from the Southern Alps, New Zealand: Earth Surface Processes and Landforms, v. 17, p. 39–51.

Bindschadler, R., 1982, A numerical model of temperate glacier flow applied to the quiescent phase of a surge-type glacier: Journal of Glaciology, v. 28, p. 239–265.

Bindschadler, R., 1983, The importance of pressurized subglacial water in separation and sliding at the glacier bed: Journal of Glaciology, v. 29, p. 3–19.
Bindschadler, R., Harrison, W. D., Raymond, C. F., and Crosson, R., 1977, Geometry and dynamics of a surge-type glacier: Journal of Glaciology, v. 18, p. 181–194.
Boulton, G. S., 1974, Processes and patterns of glacial erosion, *in* Coates, D. R., ed., Glacial geomorphology: Binghamton, New York, State University of New York, p. 41–87.
Budd, W. F., and Jenssen, D., 1975, Numerical modelling of glacier systems: International Association of Hydrological Sciences Publication No. 104, p. 257–291.
Budd, W. F., Keage, P. L., and Blundy, N. A., 1979, Empirical studies of ice sliding: Journal of Glaciology, v. 23, p. 157–170.
Chamberlin, T. C., and Chamberlin, R. T., 1911, Certain phases of glacial erosion: Journal of Geology, v. 19, p. 193–216.
Charlesworth, J. K., 1957, The Quaternary era: London, England, Edward Arnold, 1700 p.
Cotton, C. A., 1941, The shoulders of glacial troughs: Geological Magazine, v. 78, p. 113–128.
Crosby, W. O., 1928, Certain aspects of glacial erosion: Geological Society of America Bulletin, v. 39, p. 1171–1181.
Davis, W. M., 1900, Glacial erosion in France, Switzerland and Norway: Boston Society of Natural History, Proceedings, v. 29, p. 273–322.
Davis, W. M., 1906, The sculpture of mountains by glaciers: Scottish Geographical Magazine, v. 22, p. 76–89.
Doornkamp, J. C., and King, C.A.M., 1971, Numerical analysis in geomorphology: London, England, Arnold, 372 p.
Drewry, D., 1986, Glacial geologic processes: London, England, Edward Arnold, 276 p.
Embleton, C., and King, C.A.M., 1968, Glacial and periglacial geomorphology: London, England, Edward Arnold, 608 p.
Emiliani, C., 1955, Pleistocene temperatures: Journal of Geology, v. 63, p. 538–578.
Flint, R. F., 1947, Glacial geology and the Pleistocene epoch: New York, Wiley, 589 p.
Gannett, H., 1898, Lake Chelan: National Geographic, v. 9, p. 417–428.
Girard, W. W., 1976, Size, shape and symmetry of the cross-profiles of glacial valleys [Ph.D. thesis]: Iowa City, Iowa, University of Iowa, 90 p.
Glen, J. W., 1952, Experiments on the deformation of ice: Journal of Glaciology, v. 2, p. 111–114.
Glen, J. W., 1955, The creep of polycrystalline ice: Royal Society of London, Proceedings, ser. A, v. 228, p. 519–538.
Glen, J. W., and Lewis, W. V., 1961, Measurements of side-slip at Austerdalsbreen, 1959: Journal of Glaciology, v. 3, p. 1109–1122.
Graf, W. L., 1970, The geomorphology of the glacial valley cross-section: Arctic and Alpine Research, v. 2, p. 303–312.
Hallet, B., 1979, A theoretical model of glacial abrasion: Journal of Glaciology, v. 17, p. 209–221.
Hallet, B., 1981, Glacial abrasion and sliding: Their dependence on the debris concentration in basal ice: Annals of Glaciology, v. 2, p. 23–28.
Harbor, J. M., 1989, Early discoverers XXXVI: W. J. McGee on glacial erosion laws and the development of glacial valleys: Journal of Glaciology, v. 35, p. 419–425.
Harbor, J. M., 1990a, Numerical modelling of the development of glacial-valley cross sections [Ph.D. dissert.]: Seattle, Washington, University of Washington, 219 p.
Harbor, J. M., 1990b, A discussion of Hirano and Aniya's (1988, 1989) explanation of glacial-valley cross profile development: Earth Surface Processes and Landforms, v. 15, p. 369–377.
Harbor, J. M., 1992, Application of a general sliding law to simulaing flow in a glacier cross section: Journal of Glaciology, v. 38, p. 182–190.
Harbor, J. M., and Warburton, J., 1992, Glaciation and denudation rates: Nature, v. 356, p. 751.
Harbor, J. M., and Wheeler, D., 1992, On the mathematical description of glaciated-valley cross sections: Earth Surface Processes and Landforms, v. 17, p. 477–485.
Harbor, J. M., Hallet, B., and Raymond, C., 1988, A numerical model of landform development by glacial erosion: Nature, v. 333, p. 347–349.
Hirano, M., 1981, An explanation of the U-shaped profile of the glacier valley based on the variation principle: Bulletin of Faculty of Literature (Jinbun-Kenkyu), Osaka City University, v. 33, no. 4 (Geography), p. 1–14.
Hirano, M., and Aniya, M., 1988, A rational explanation of cross-profile morphology for glacial valleys and of glacial valley development: Earth Surface Processes and Landforms, v. 13, p. 707–716.
Hirano, M., and Aniya, M., 1989, A rational explanation of cross-profile morphology for glacial valleys and of glacial valley development: A further note: Earth Surface Processes and Landforms, v. 14, p. 173–174.
Hirano, M., and Aniya, M., 1990, A reply to "A discussion of Hirano and Aniya's (1988, 1989) explanation of glacial-valley cross profile development" by Jonathan M. Harbor: Earth Surface Processes and Landforms, v. 15, p. 379–381.
Hodge, S. M., 1974, Variations in the sliding of a temperate glacier: Journal of Glaciology, v. 13, p. 349–369.
Hodge, S. M., 1985, Two-dimensional, time-dependent modeling of an arbitrarily shaped ice mass with the finite-element technique. Journal of Glaciology, v. 31, p. 350–359.
Hooke, R. L., Raymond, C. F., Hotchkiss, R. L., and Gustafson, R. J., 1979, Calculations of velocity and temperature in a polar glacier using the finite-element method: Journal of Glaciology, v. 24, p. 131–146.
Humphrey, N. F., 1987, Basal hydrology of a surge-type glacier: Observations and theory relating to Variegated glacier [Ph.D. thesis]: Seattle, Washington, University of Washington, 227 p.
Iken, A., 1981, The effect of the subglacial water pressure on the sliding velocity of a glacier in an idealized numerical model: Journal of Glaciology, v. 27, p. 407–421.
Iverson, N. R., 1990, Laboratory simulations of glacial abrasion: Comparison with theory: Journal of Glaciology, v. 36, p. 304–314.
Iverson, N. R., 1991, Potential effects of subglacial water-pressure fluctuations on quarrying: Journal of Glaciology, v. 37, p. 27–36.
Johnson, A., 1970, Physical processes in geology: San Francisco, California, Freeman, Cooper & Co., 577 p.
King, C.A.M., 1974, Morphometry in glacial geomorphology, *in* Coates, D. R., ed., Glacial Geomorphology: Binghamton, New York, State University of New York, p. 147–162.
Lewis, W. V., 1947, Cross sections of glaciated valleys: Journal of Glaciology, v. 1, p. 37–39.
Lewis, W. V., 1954, Pressure release and glacial erosion: Journal of Glaciology, v. 2, p. 417–422.
Linton, D. L., 1963, The forms of glacial erosion: Institute of British Geographers Transactions, v. 33, p. 1–28.
Lliboutry, L., 1968, General theory of subglacial cavitation and sliding of temperate glaciers: Journal of Glaciology, v. 17, p. 21–58.
Lliboutry, L., 1979, Local friction laws for glaciers, a critical review and new openings: Journal of Glaciology, v. 23, p. 67–95.
Mahaffy, M. W., 1976, A three-dimensional numerical model of ice sheets: Test on the Barnes Ice Cap, Northwest Territories: Journal of Geophysical Research, v. 81, p. 1059–1066.
Matthes, F. E., 1930, Geologic history of the Yosemite valley: U.S. Geological Survey Professional Paper 160, 137 p.
McGee, W J, 1883, Glacial cañons: Science, v. 2, p. 315–316.
McGee, W J, 1894, Glacial cañons: Journal of Geology, v. 2, p. 350–364.
Molnar, P. and England, P., 1990, Late Cenozoic uplift of mountain ranges and global climate change: chicken or egg?: Nature, v. 346, p. 29–34.
Molnar, P. and England, P., 1992, Reply to Summerfield, M. A. and Kirkbride, M. P. (1992) Climate and landscape response: Nature, v. 355, p. 306.
Murray, D. R., and Locke, W. W., 1989, Dynamics of the late Pleistocene Big Timber Glacier, Crazy Mountains, Montana, U.S.A.: Journal of Glaciology, v. 35, p. 183–190.
Nye, J. F., and Martin, P.C.S., 1968, Glacial erosion: International Association of Hydrological Sciences Publication No. 79, p. 78–85.
Oerlemans, J., 1984, Numerical experiments on large-scale glacial erosion: Zeitschrift für Gletscherskunde und Glazialgeologie, v. 20, p. 107–126.
Paterson, W.S.B., 1981, The physics of glaciers: Oxford, England, Pergamon Press, 380 p.
Pierce, K. L., 1979, History and dynamics of glaciation in the northern Yellowstone National Park area: U.S. Geological Survey Professional Paper 729-F.
Raymond, C. F., 1971, Flow in a transverse section of the Athabasca Glacier, Alberta, Canada: Journal of Glaciology, v. 10, p. 55–84.
Raymond, C. F., 1978, Numerical calculation of glacier flow by finite element methods. Final technical report for National Science Foundation Grant No. DPP74-19075: Seattle, Washington, University of Washington, 230 p.
Raymond, C. F., and Harrison, W. D., 1987, Fit of ice motion models to observations from Variegated Glacier, Alaska, *in* Waddington, E. D., and Walder, J. S., eds., The physical basis of ice sheet modelling: International Association of Hydrologic Sciences Publication 170, p. 153–166.
Reynaud, L., 1973, Flow of a valley glacier with a solid friction law: Journal of Glaciology, v. 12, p. 251–258.
Roberts, M. C., and Rood, K. M., 1984, The role of ice contributing area in the morphology of transverse fjords, British Columbia: Geografiska Annaler, v. 66A, p. 381–393.
Röthlisberger, H., 1972, Water pressure in intra- and subglacial channels: Journal of Glaciology, v. 11, p. 177–203.
Röthlisberger, H., and Iken, A., 1981, Plucking as an effect of water-pressure variations at the glacier bed: Annals of Glaciology, v. 2, p. 57–62.
Shackleton, N. J., and Opdyke, N. D., 1973, Oxygen isotope and paleomagnetic stratigraphy of equatorial Pacific core V28-238: Oxygen isotope temperatures and ice volumes on a 10^5 and 10^6 year scale: Quaternary Research, v. 3, p. 39–55.
Shoemaker, E. M., 1986, The formation of fjord thresholds: Journal of Glaciology, v. 32, p. 65–71.
Shoemaker, E. M., 1988, On the formulation of basal debris drag for the case of sparse debris: Journal of Glaciology, v. 34, p. 259–264.
Summerfield, M. A., and Kirkbride, M. P., 1992, Climate and landscape response: Nature, v. 355, p. 306.
Svennson, H., 1958, Morphometrischer Beitrag zur Charakterisierung von Glazialtälern: Zeitschrift für Glestcherskunde und Glazialgeologie, v. 4, p. 99–105.
Svennson, H., 1959, Is the cross-section of a glacial valley a parabola?: Journal of Glaciology, v. 3, p. 362–363.
Tricart, J., and Cailleux, A., 1962, Le modèle glaciare et nival: Paris, France, Sedes, 508 p.
Wheeler, D. A., 1984, Using parabolas to describe the cross-sections of glaciated valleys: Earth Surface Processes and Landforms, v. 9, p. 391–394.

MANUSCRIPT RECEIVED BY THE SOCIETY SEPTEMBER 5, 1991
REVISED MANUSCRIPT RECEIVED FEBRUARY 26, 1992
MANUSCRIPT ACCEPTED MARCH 2, 1992

Printed in U.S.A.